INTRODUCTION

TISSUE INJURY MODELS are commonly employed to investigate stem/prognitor cell systems. Tissue damage stimulates stem/progenitor cells to participate in repopulation. There are many experimental injury models in various organs including the liver and the pancreas. The Solt-Farber liver injury model is a representative example; hepatic injury caused by chemicals or partial hepatectomy are treated with 2-acetylaminofluorene (2-AAF) to induce the proliferation of hepatic oval cells from the portal triad in the hepatic lobules (Golding et al., 1995; Yasui et al., 1997). Hepatic oval cells have been demonstrated to be progenitors for hepatocytes, bile duct cells, and also for pancreatic endocrine cells (Dabeva et al., 1997). Another example is obstruction of the common bile duct leading to liver injury, and as a result, the appearance of c-Kit-positive cells producing α-fetoprotein (Omori et al., 1997; Yang et al., 2002). These cells are thought to be one of the precursors of liver cells. In the pancreas, ligation of the main pancreatic duct leads to marked reduction of acinar cells (Abe and Watanabe, 1995), a phenomenon accompanied by the proliferation of small epithelium with duct-like structures (Takahashi et al., 1998). Insulin or glucagon-producing cells have been found among these duct-like structures, indicating dysregulated differentiation of pancreatic cells (Wang et al., 1995). These findings indicate that tissue stem cells are activated by tissue injury, and tissue injury models are effective for the induction of efficiently proliferating tissue progenitor cells.

In the salivary gland with ligation of the main excretory duct, acinar cells had receded within 7 to 10 days, and a marked proliferation of small epithelium was observed (Takahashi et al., 1998; Walker, 1987; Walker and Gobe, 1987). After ligation of the duct, almost all the acinar cells receded and small epithelial cells with a duct-like structure (ductal proliferation) were observed in mice and rats. Reopening of the obstructed duct resulted in regeneration of normal gland tissues. During the regeneration process, the duct cells proliferate and differentiate into acinar cells within 5 days after the reopening. Intercalated duct cells may be precursors for both duct epithelial and acinar cells. We considered that the proliferated small epithelial cells contained stem/progenitor cells. We previously reported isolating the progenitor cells from the duct-ligated submandibular glands of mice and rats (Hisatomi et al., 2004; Okumura et al., 2003), which were designated as salivary gland-derived progenitor cells (mouse SGP-1 and rat SGP-1). The rat SGP-1 cells were positive for both CD49f and intracellular laminin. In the duct-ligated submandibular gland of rats, the proliferated small-epithelial cells included CD49f+/intracellular laminin+ cells. In the duct-ligated salivary gland of mice, the proliferated small-epithelium cells included Sca-1+/c-Kit+ cells. To demonstrate that the proliferated small epithelial cells included the stem/progenitor cells, the Sca-1+/c-Kit+ fraction from adult mice salivary glands was sorted by means of fluorescence-activated cell sorting. The sca-1+/c-Kit+ cells were positive for CD49f and intracellular laminin, and differentiated into both hepatic and pancreatic–endocrine–phenotypic cells *in vitro*. After transplantation into the injured liver, the transplanted mSGP-1 cells completely integrated into hepatic cords. The mouse SGP-1 cells differentiated into hepatic phenotypes. In this study, we investigated the same progenitors in the swine salivary gland as the rat and mouse salivary glands.

MATERIALS AND METHODS

Cell isolation and culture

We isolated cells from the salivary glands of male (Landress-Dyrock) swine (body weight 7–10 kg, age 3 to 4 weeks) by ligating/or nonligating the main conduit ducts of the submandibular glands. The protocol was approved by the Center for Animal Resources and Development of Kumamoto University. Animal care was performed as outlined in the Guide for Care and Use of Laboratory Animals. When ligating ducts or resecting glands, the pigs were anesthetized as follows. Initial sedation was obtained with a deep intramuscular injection (forequarter paraspinal muscle) of azaperone (1–5 mg/kg, Sankyo Co., Tokyo, Japan) and ketamine hydrochloride (10–20 mg/kg, Sankyo Co.). The pigs were then washed with a solution of aqueous iodine solution and taken into the operation of the latter. The removed glands were minced and incubated with 30 mL of EGTA buffer (Hisatomi et al., 2004; Okumura et al., 2003) at 37°C for 20 min, then cen-

trifuged at $100 \times g$ at room temperature for 5 min. Pellets were suspended with 50 mL digestion medium containing D-MEM/F12 1:1(Gibco Invitrogen Co., Grand Island, NY), 1.67 mg/mL collagenase (Gibco), 1.33 mg/mL hyaluronidase (Nacalai Tesque, Tokyo, Japan), and incubated at 37°C for 40 min. The tissues were dispersed into single cells with dispersion medium containing D-MEM/F12 1:1, 1.67 mg/mL dispase (Gibco) and incubated at 37°C for 60 min. The cells were then passed through a stainless filter and centrifuged at $100 \times g$ for 5 min at 4°C. The pellets were suspended with 10 mL D-MEM/F12 1:1 medium, washed three times with serum-free Williams' medium E (Gibco), then placed on 100 mm type I collagen-coated dishes (Asahi Techno Glass, Chiba, Japan) with Williams' medium E supplemented with 10% fetal bovine serum (FBS) (Gibco), 20 ng/mL recombinant human EGF (Sigma-Aldrich, St. Louis, MO), 10^{-6}mol/L dexamethasone (Sigma Chemical Co., St. Louis, MO), 100 U/mL penicillin G, and 100 μg/mL streptomycin (Gibco). Colonies were extracted using a cloning ring (Asahi Techno Glass).

Differentiation study

For differentiation, cultured cells during passages 7 to 15 were suspended in our differentiation medium and cultured for 14 days. Next, these cells plated with densities of 1000 cell/well in 96-well U-bottom plates (Sumitomo Bakelite Co., Ltd., Tokyo, Japan) for spherical culture. Cells were cultured in a 37°C, 5% CO$_2$ incubator. Medium was changed every 3 days. For induction of hepatic lineage, the differentiation culture medium used was Williams' medium E supplemented with 10% FBS, 10 mmol/L nicotinamide (Sigma Chemical), 10^{-6} mol/L dexamethasone (Sigma Chemical), 100 U/ml penicillin G, and 100 μg/mL streptomycin (Gibco). For induction of pancreatic lineage, the differentiation medium was Williams' medium E supplemented with 10% FBS, 10 mmol/L nicotinamide, and 20 nmol/L of glucagon-like peptide-1 (GLP-1; Sigma Chemical), 10^{-6} mol/L dexamethasone (Sigma Chemical), 100 U/ml penicillin G, and 100 μg/mL streptomycin (Gibco).

Preparation of control pancreatic endocrine cells and hepatocyte cells

Control pancreatic endocrine cells obtained by the autodigestion method, as described previously (Ohgawara et al., 1994, 1998), were suspended in conditional medium (10% FBS, 11 mmol/L D-glucose, 10 mmol/L nicotinamide in RPMI-1640) and divided into several aliquots. Each aliquot of cells was cultured in 25-mm^2 culture flasks (Sumitomo Bakelite) in a humidified incubator at 37°C with 5% CO$_2$. The control cells were incubated for 10 more days and then treated with 0.05% trypsin/EDTA solution (Invitrogen, Carlsbad, CA). The dispersed cells were collected and resuspended in conditional medium and cultured in 30-mm^2 tissue culture dishes (Sumitomo Bakelite) or 30-mm^2 tissue culture plates at a density of 5.0×10^4 cells/500 μL. On day 3, the medium was changed to RPMI-1640 containing 10% FBS and 11 mmol/L D-glucose, and the cells were then ready for use in the following insulin secretory test and quantification of the mRNA for insulin.

Livers were excised and the left lateral lobe removed. Hepatocytes were isolated by a two-step collagenase digestion procedure essentially as previously described (Capelna et al. 2003; Fernández-Fígares et al. 2004), where only a small portion (approximately 80 g) of the lateral lobe was used. Hepatocytes were seeded into T-25 flasks, precoated with pig tail collagen and cultured as previously described (Richards and Poch, 2002). Briefly, cells were initially maintained in William's medium E containing insulin–transferrin–selenium (ITS) and 10% FBS. Following a 3-h attachment period, flasks were washed with HEPES-buffered saline. William's medium E containing 5% FBS with ITS was added to each flask. On the following day, flasks were washed twice and media was replaced with serum-free William's E basal medium containing 10 nM dexamethasone, 100 μM 2-mercaptoethanol, 10 mM HEPES, 10 nM Na$_2$SeO$_3$, 2 mM glutamine, antibiotics, 0.01% DMSO, 0.1% BSA and 1 ng/mL bovine insulin. These hepatocyte cells were used for quantification of the mRNA expression for albumin.

Insulin release

The cells on type I collagen were cultured with the differentiation medium for 14 days. Next, the cells were seeded in 96-well U-bottom plate and cultured for 7 to 10 days. Glucose-stimulated insulin secretion was measured on days 7 to 10 of spherical culture. First, the cells were incubated in RPMI-1640 containing 3.3 mmol/L D-glucose

and 10% FBS for 30 min, then FBS was changed to 0.1% bovine serum albumin BSA. The protocol for the glucose-stimulation test was described (Nagai et al., 2004). The secretory responsiveness of the cells to glucose (20 mmol/L D-glucose) and potassium (20 mmol/L) was determined during 60-min incubation. After incubation, the medium was collected and centrifuged at 3000 rpm to store at −20°C for insulin assay.

Insulin assay

The sample medium collected during the incubation period was centrifuged at 10,000 rpm for 15 sec, and the supernatant was stored at −20°C until assay. The assay was performed using the method of Mercodia porcine insulin ELISA (Mercodia AB, Uppsala, Sweden) soon after the sample was thawed. The number of cells were corrected in both group.

Reverse-transcription PCR analysis

Total RNA was extracted using an RNAeasy micro kit (Qiagen GmbH, Germany) according to the manufacturer's protocol. In our hands, this protocol always yielded RNA without significant genomic DNA contamination. Complementary DNAs were prepared from 1 μg of total RNA using the ThermoScript RT-PCR system (Invitrogen) with oligo-dT primers, according to the manufacturer's instructions. The resulting cDNA was amplified using GeneAmp PCR 9700 (Perkin-Elmer Corporation, Norwalk, CT) with the following sets of primers: for GATA6 (178-bp fragment), forward 5'-CTGTCCCCATGACTCC-AACT-3' and reverse 5'-ATGTACAGCCCGTC-TTGACC-3' (Gillio-Meina et al., 2003); for PDX-1 (102-bp fragment), forward 5'-CGCGGCCTA-GAGATGTATTT -3', and reverse 5'-CGCGGCC-TAGAGATGTATTT-3; -3 for PAX-6 (402-bp fragment), forward 5'-CAGCCCTCACCAACACC-TAC-3' and reverse 5'-CGCCCAACTGTTGTG-TCC-3'; for insulin (233-bp fragment), forward 5'-AGGCCTTCGTGAACCAGCAC-3' and reverse 5'-GAGGGAACAGATGCTGGTGC -3'; for somatostatin (284-bp fragment), forward 5'-TCTC-CATCGTCCTGGCTC-3' and reverse 5'-ATTC-TTGCAGCCAGCTTTG-3'; for glucagon (227-bp fragment), forward 5'-GACAAGCGCCACTCA-CAG-3' and reverse 5'-TTCACCAGCCAAGCA-ATG-3', for albumin (194-bp fragment), forward 5'-CTGCACAGAGTCCTTGGTGA-3', and re-

verse 5'-CTGTTGCATGAGGCTTGTGT-3'; for AFP (205-bp fragment), forward 5'-CCTTATCA-TCGGGCAGTTGT-3', and reverse 5'-TTGCAGT-GCTACACCCTGAG-3'; and for GAPDH (452-bp fragment), forward 5'-ACCACAGTCCATGCCA-TCATCAC-3' and reverse 5'-TCCACCACCCT-GTTGCTGTA-3'. PCR amplification conditions were 1 min at 98°C followed by 30 cycles of 98°C for 10 sec, 53°C to 57°C for 15 sec, 72°C for 15 to 50 sec. PCR products were electrophoresed on a 4% NuSieve GTG agarose gel (FMC Bioproducts, Rockland, ME), and visualized with ethidium bromide (Nacalai).

Real-time polymerase chain reaction

For quantification of insulin and PDX-1 mRNAlevels in the PE cells, the real-time polymerase chain reaction (PCR) (Perkin-Elmer) method was used. Specific primers for porcine insulin and albumin were designed using Primer Express Software (Applied Biosystems, Bedford, MA) as follows: porcine insulin forward; 5'-AGCGCGG-CTTCTTCTACA-3' and reverse; 5'-CACCTGCC-TGAGGGTTCT-'3, porcine albumin forward; 5'-ACGCCCCAGAACTCCTTTAT-3' and reverse; 5'-GGCAGCTTTATCAGCAGCTT-3'. The two-step amplification method was applied to semi-quantification of mRNA expression with SYBER Green PCR reagents and an ABI 7500 Real-Time PCR System (Applied Biosystems), according to the manufacturer's instructions. Total RNA isolation with DNAse was previously described. Complementary DNAs were prepared from 1μg of total RNA using the ThermoScript RT-PCR system (Invitrogen) with random hexamer primers, according to the manufacturer's instructions. Reactions were performed using 1.0 μL cDNA and 25 μL SYBR Green PCR Master Mix (2×) in a reaction volume of 50 μL. The PCR amplification conditions were as follows: step 1, 1 min at 50°C; step 2,10 min at 95°C; and step 3, 40 cycles with heating to 95°C for 15 sec and cooling to 60°C for 1 min, and adding a dissociation stage. cDNA levels were normalized to levels of glyceraldehyde-3-phosphate dehydrogenase (GAPDH). For porcine GAPDH quantification, specific primers were synthesized as follows: forward, 5'-CCAG-AACATCATCCCTGCTT-3' and reverse 5'-AG-ATCCACAACCGACACGTT-3'. Electrophoretic analysis of expected product sizes was performed for all primer sets prior to two-step, real-time RT-PCR to confirm the reaction fidelity.

Histological analysis and immunofluorescent staining of cultured cells

For histological analysis, the swine salivary glands were fixed in 10% formaldehyde and embedded in paraffin. Sections were stained with hematoxylin-eosin or PAS. Cells were cultured on a glass based dish (Asahi Techno Glass). After three times washing with phosphate buffered-saline (PBS), cells were fixed in 4% paraformaldehyde (Nacalai) for 20 min at 4°C, then washed in PBS containing 0.2% polyoxyethylene 20 sorbitan mono-laurate (Tween 20) (Wako Pure Chemical Inc., Osaka, Japan). Nonspecific binding was blocked with nonimmune serum of the species from which the secondary antibody had been obtained or a nonspecific staining blocking reagent (DAKO cytometion Glostrup, Denmark). The primary antibodies used in this study were antihuman CD49f, antihuman laminin, antihuman lamininα1, antihuman albumin, antihuman AFP, antiswine insulin, antiporcine glucagon, antihuman GATA6, antihuman CK8, antihuman CK18, and antihuman CK19. Further information on applied antibodies is given in Table 1. The secondary antibodies used were Alexa488-conjugated antirabbit IgG, antimouse IgG, or Alexa594-conjugated antiguinea pig IgG (Molecular Probes, Inc. Eugene, OR). Stained cells were viewed under a confocal laser-scanning microscope model FV500 (Olympus Optical Ltd., Tokyo).

Analysis of cell-surface antigens

Cells were stained and analyzed by flow cytometry, as described (Hisatomi et al., 2004; Okumura et al., 2003). In brief, cultured cells were collected after trypsin-EDTA (Invitrogen) treatment. Sample cells were washed three times with staining buffer, and then incubated with various primary antibodies. The antibodies (Santa Cruz Biotechnology, Inc., Santa Cruz, CA) used were mouse IgG1 and IgG2a isotype control, antihuman CD29, antihuman CD34, antiporcine CD44, antiporcine CD45, antihuman CD49c, antihuman CD49f, antihuman CD90 (Thy-1), and antihuman c-kit (CD117). Further information of antibodies is given in Table 1. The secondary reagents we used were Alexa488-conjugated antimouse IgG or antirat IgG (Santa Cruz Biotechnology, Inc.). Cells were washed three times with staining buffer and analyzed. VIA-PROBE (BD Biosciences, San Jose, CA) was used to discriminate living from dead cells, which were excluded by flow-cytometric analysis. Labeled cells were analyzed using a FACS calibur flow cytometer (BD Biosciences).

RESULTS

A common feature of rat, mouse, and swine salivary gland tissue is that it consists of PAS-positive acinar cells, PAS-negative duct epithelial

TABLE 1.   DETAILS OF THE APPLIED ANTIBODIES

Antigen	Host	Product number	Manufacturer
Laminin	Rabbit, polyclonal	Z0097	DAKO
Albumin	Rabbit, polyclonal	Z0002	DAKO
AFP	Goat, polyclonal	A0012	DAKO
Insulin	Guinea pig, monoclonal	N1542	DAKO
Glucagon	Rabbit, polyclonal	A0565	DAKO
Somatostatin	Goat, polyclonal	sc-7819	Santa Cruz
Pancreatic polypeptide	Rabbit, polyclonal	7100-0104	SEROTEC
GATA-6	Rabbit, polyclonal	sc-9055	Santa Cruz
CD29	Mouse, monoclonal	M0889	DAKO
CD34	Mouse, monoclonal	CBL496	SEROTEC
CD44	Rat, monoclonal	MCA1449	SEROTEC
CD45	Mouse, monoclonal	MCA1447	SEROTEC
CD49c	Mouse, monoclonal	AB1920	CHEMICON
CD49f	Rat, monoclonal	555734	BD Biosciences
CD90(Thy-1)	Mouse, monoclonal	555593	BD Biosciences
CD117(c-kit)	Rabbit, polyclonal	sc-5535	Santa Cruz
CK8	Mouse, Monoclonal	RE1104C100	BioVendor
CK18	Mouse, monoclonal	61028	PROGEN
CK19	Mouse, monoclonal	61029	PROGEN
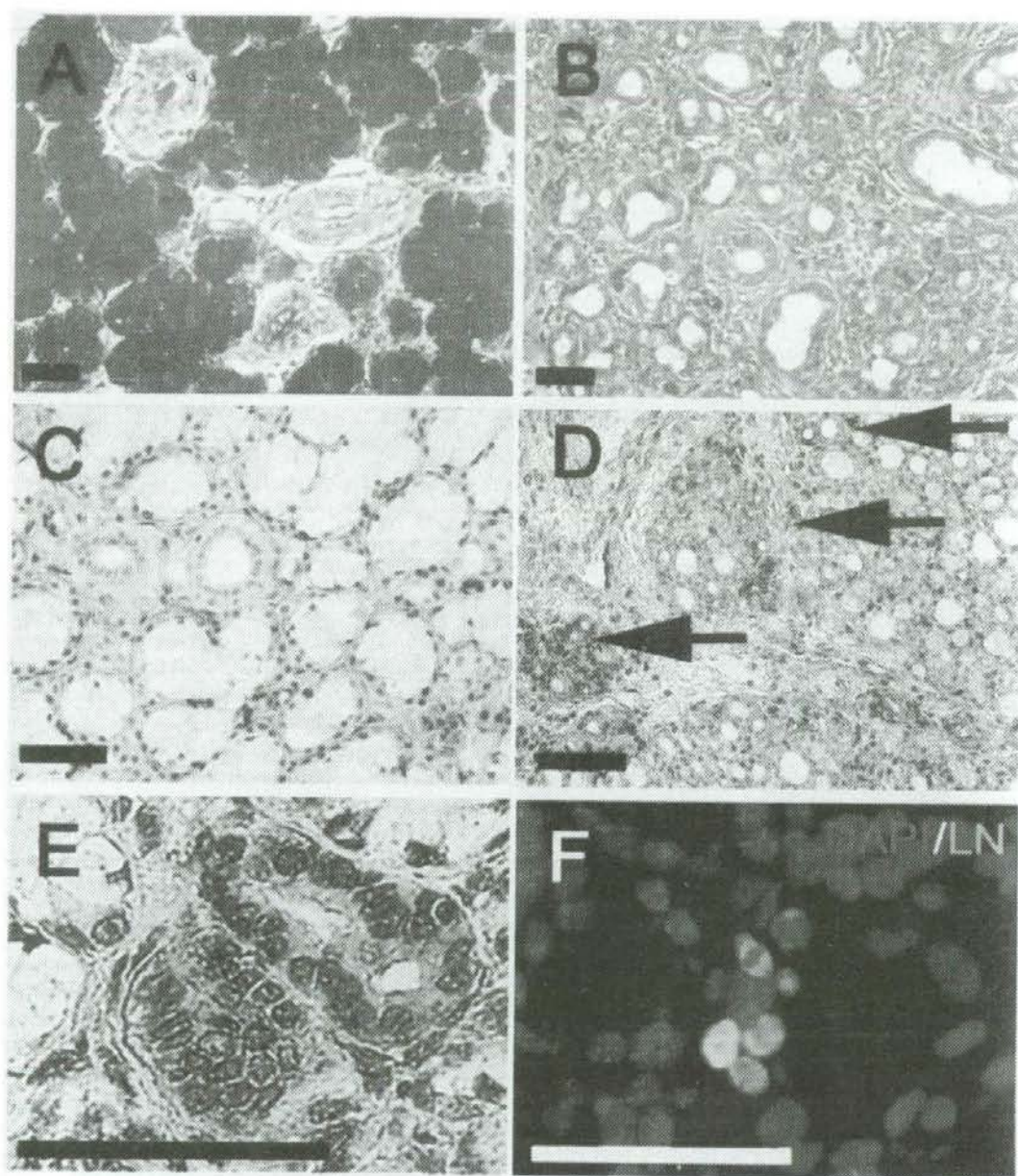
FIG 1. Histological analysis of submandibular glands. (A,B) PAS staining of submandibular gland were performed with a swine (A) before and (B) 10 days after duct ligation. (B) Ductal proliferation and disappearance of PAS-positive acinar cells occurred after ligation of main excretory duct. (C–F) Salivary glands (C) before and (D–F) after duct ligation were stained with laminin antibody. (C) In the intact salivary glands, the localization of laminin is evident in the basement membranes of the excretory duct and surrounding the acinus. (D) Clusters of proliferated small epithelial cells were positive for laminin, and these intracellular laminin-positive cells were found in the ductal and periductal areas (arrow). (E,F) High magnification of the same ligated salivary gland stained with laminin antibody by immunohistochemistry (E) and immunofluorescence (F). (F) Intracellular laminin-positive cells (green) were observed in clusters of small epithelial cells. Scare bars = 100 mm.

cells, and PAS-negative myoepithelial cells (Fig. 1A). Seven to 10 days after ligation of the main excretory duct, almost all acinar cells had receded and been replaced by proliferating small duct epithelial cells (Fig. 1B). The phenomenon is called "ductal proliferation." In previous studies, we demonstrated that CD49f-positive and intracellular laminin-positive cells are induced by ligation of the duct in rats (Okumura et al., 2003) and mice (Hisatomi et al., 2004), and these cells have the capacity to differentiate into hepatic and pancreatic cell lineages. In duct-ligated submandibular glands of swine, CD49f- and intracellular laminin-positive cells were observed among the clusters of small cells in the periductal areas (Fig. 1D).

We prepared salivary gland cells as described in Materials and Methods. Various cell types appeared on the dish, and fibroblast-like cells and large epithelium-like cells were predominant (Fig. 2A–C). The fibroblast-like cells and large epithelium-like cells were negative for amylase, intracellular laminin, CK8, CK18, and CK19, but 40–60% of the cells were positive for CD49f (Table 2). All the cells which originated from fibroblast-like cells and large epithelium-like cells were unable to differentiate into any phenotypes by spherical- and gel-culture (data not shown). After 10–16 days, colonies of cells (20–100 cells) with a small and round epithelium-like shape appeared. One to five colonies of 1×10^4 plated cells were formed. These colonies included CD49f-positive cells (100%, Fig. 2D), intracellular laminin-positive cells (100%, Fig. 2E), CK19-positive cells (90.1 ± 3.7%), and CK18-positive cells (22.2 ± 1.3%), and these cells, which were repeatedly obtained from different rat salivary glands using the same protocol, exhibited the same morphology and characteristics. These colonies were plated on type I collagen-coated 24-well plates for further purification. The extracted cells were purified individually with limiting dilution on type I collagen-coated 96-well plates.

The single purified cells were designated as "swine salivary gland–derived progenitor" swine SGP (Fig. 4A) and used for further experiments. All experiments were performed using cells at 7 and 15 passages because the swine SGP cells were immature and homogeneous after single-cell purification. Swine SGP cells were positive for CD49f, intracellular laminin, AFP, and CK18 (Fig. 2F–H), and negative for CK19, CK8, CK7, insulin, glucagon, albumin, and AAT (Table 2). The doubling time of SGP cells is approximately 46 h. SGP-1 cells grew for at least 3 months after the initial purification and without change in shape or characteristics. The doubling time of the swine SGP cells was prolonged after 20 to 60 passages.

Flow-cytometric analysis of swine SGP cells cultured on type I collagen (Fig. 3) demonstrated that the cells were positive for CD29, CD44, CD49f, c-Kit, and Thy-1. With regard to the integrins, a portion of swine SGP cells were positive for CD49f, CD29, and CD49c. When cultured on type I collagen-coated plates, swine SGP cells formed small clusters (Fig. 4A). The results of immunofluorescent staining of these small clusters and spheroids cultured in a 96-well U-plate for 2 weeks are shown in Figure 4B–E. Most spheroids expressed albumin and insulin. Swine SGP cells were suspended in the differentiation medium (contained with 10 mmol/L nicotinamide and/or 10 mmol/L GLP-1) and then were plated with densities of 1000 cells/well in 96-well plates. Seven days after plating, spheroid bodies were analyzed by RT-PCR (Fig. 4G) for GATA6, AFP, albumin, PDX-1, insulin, glucagon, and immunofluorescent staining (Fig. 4A–F) for albumin (red), somatostatin (red), pancreatic polypeptide (red), glucagon (red) and insulin (green) expression. Transcripts for albumin, Pdx-1, glucagon, and insulin were not detected in monolayer cells (Fig. 4G). Meanwhile, AFP was expressed in monolayer cells. After 14 days, we detected transcripts of albumin and AAT (data not shown) in spheroid bodies cultured in differentiation

FIG. 2. Configuration and immunohistochemistry of cells in primary culture and purified SGP cells. (A) fibroblast-like cells, (B) large epithelium-like cells, and (C) small epithelium-like cells were observed in primary culture. (C) Swine SGP cells originated from small epithelium-like cells were purified. Polygonal forms revealed by phase contrast of swine SGP cells cultured on type I collagen. (D,E) In primary culture, small epithelium-like cells were positive for CD49f (D; green) and intracellular laminin (E; green). (F) Swine SGP cells after purification were stained with laminin and CD49f by treatment with Tween 20. Intracellular laminin (red) was detected in all the cells, and cell-surfaces were positive for CD49f (green). (G,H) Swine SGP cells were positive for GATA6 (G), AFP (H) by immunostainting. (D–H) Nuclei were stained with 4,6-diamidino-2-phenylindole. Scale bars: A–H, 100 mm.
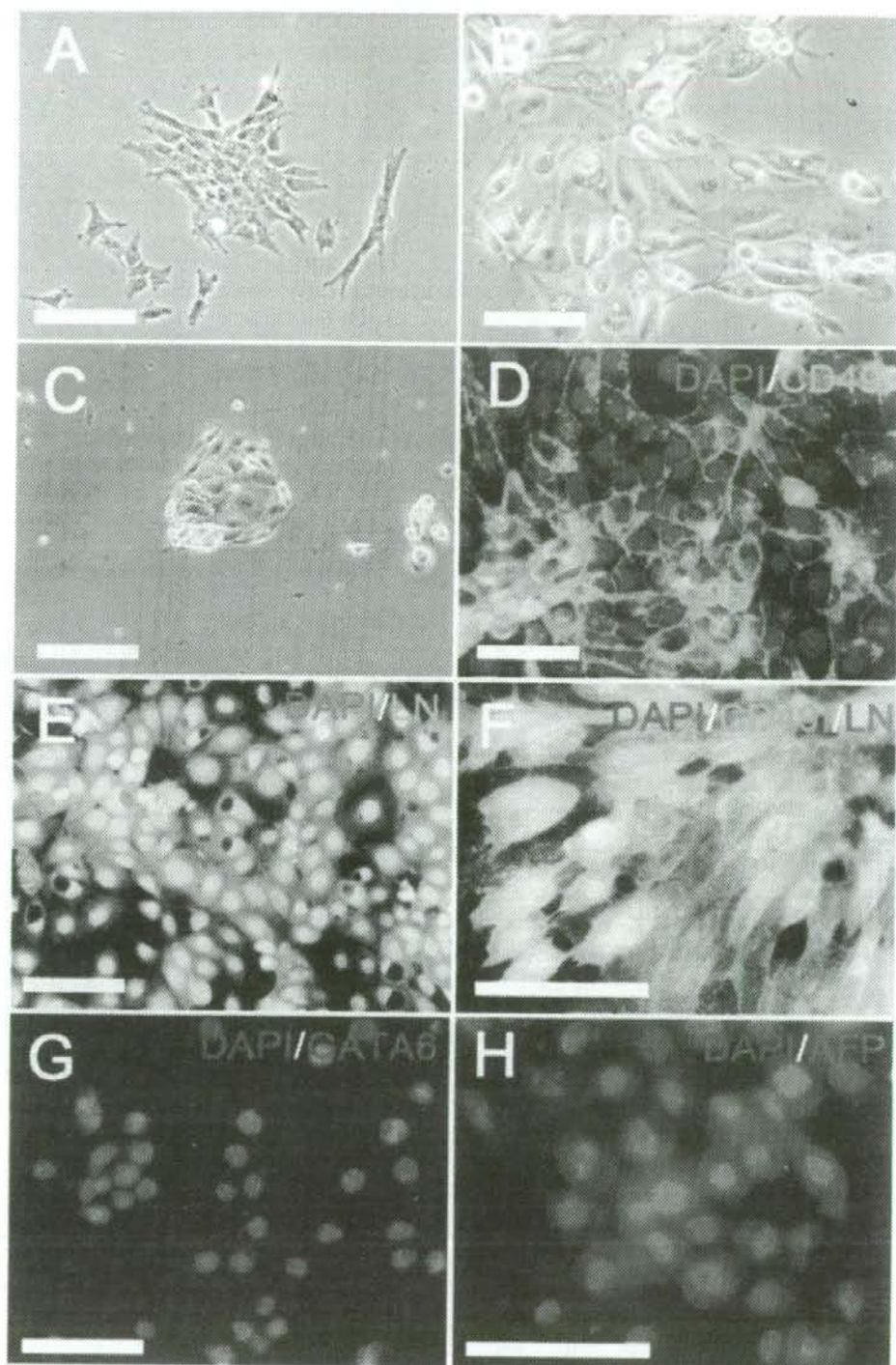
FIG. 2.

TABLE 2. MARKERS OF CELLS IN PRIMARY CULTURE

	Amylase	CD49f	Intracellular laminin	CK8	CK18	CK19	CK20
Fibroblast-like cells	0	60.6 ± 3.1^a	0	0	0	23.7 ± 2.6^c	0
Large epithelium-like cells	0	27.8 ± 2.1^b	0	0	0	0	0
Small epithelium-like cells	0	$100^{a,b}$	100	0	22.2 ± 1.3	90.1 ± 3.7^c	0

There were fibroblast-like cells, large epithelium-like cells, and small and round epithelium-like cells in primary culture. These cells were extracted and further purification. Fibroblast-like cells and large epithelium-like cells were negative for amylase, intracellular-laminin, CK8, CK18, and CK19. CD49f-positive cells, which are a marker of SGP cells, were $60.6 \pm 3.1\%$ of these cells. However, fibroblast-like cells and large epithelium-like cells could not differentiate into any phenotypes. The small and round epithelium-like cells were positive for CD49f, intracellular laminin, CK19, AFP, and partially CK18. CK19 expression was receded and CK18 expression was preceded.

[a]$p < 0.05$.
[b]$p < 0.05$.
[c]$p < 0.05$.
Mean SD, $n = 10$.

medium for hepatic lineages. Gene expression of PDX-1, glucagon, and insulin was detected in spheroid bodies cultured in the differentiation medium for pancreatic lineages. A cluster of somatostatin immunoreactive cells were detected in a spheroid body, and pancreatic–polypeptide immunoreactive cells were scattered in a spheroid (Fig. 4E–F). We examined an insulin-releasing test stimulated by glucose and potassium. The results of insulin response to glucose and potassium are shown in Figure 5. With 3.3 mmol/L D-glucose,

the positive control porcine endocrine cells (porcine PE cells), spheroid bodies of swine SGP cells, and SGP cells on type I collagen released 0.13 ± 0.05, 0.02 ± 0.01, and <0.003 (not detected) ng/mL/1×10^5 cells insulin, respectively. When the D-glucose concentration increased to 20 mmol/L, the insulin secretion of each group was 1.7 ± 0.23, 0.17 ± 0.03, 0.14 ± 0.02 ng/mL/1×10^5 cells, respectively ($p < 0.05$). With potassium-stimulated insulin secretion (3.3 mmol/L D-glucose and 50 mmol/L KCl), the control
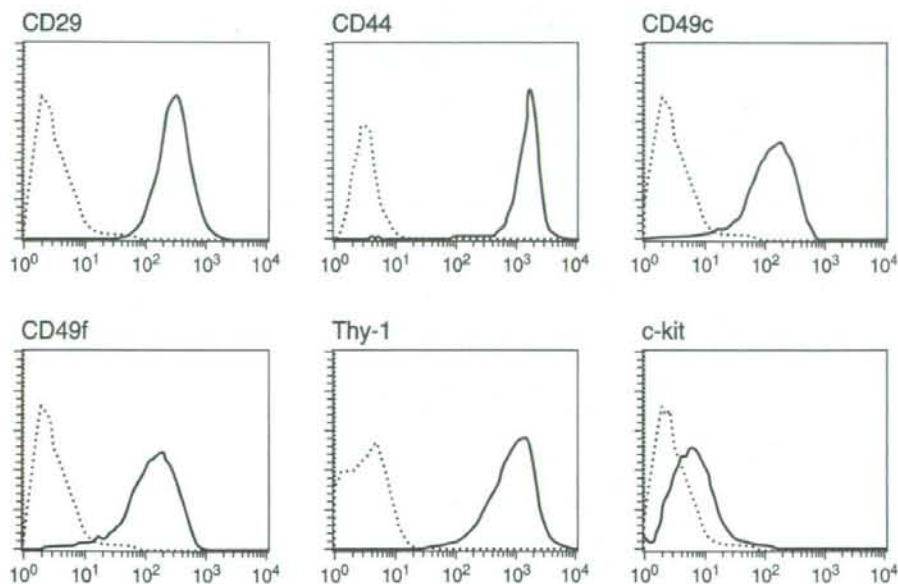

FIG. 3. Flow cytometric analysis of ligated salivary gland-derived progenitors. Continuous lines represent histograms using antibodies for each surface marker. Dotted lines represent isotype control antibody treatment.

porcine PE cells, spheroid bodies of swine SGP cells and SGP cells on type I collagen released 0.7 ± 0.02, 0.14 ± 0.04, and 0.09 ng/mL/1×10^5 cells insulin, respectively. Expression of porcine insulin and albumin mRNA was confirmed by real-time quantitative PCR (Fig. 6). Porcine-specific primers for insulin, albumin, and GAPDH were synthesized. After spherical culture was started, gene expression of insulin and albumin was significantly increased (five-fold) and that of insulin was also increased (3.8-fold) with differentiation medium with nicotinamide and/or GLP-1 treatment in spherical culture. The expressions of albumin and insulin were 1/10-fold and

1/4-fold compared to control cells (porcine hepatocyte for albumin, porcine pancreatic endocrine cells for insulin).

We investigated the intracellular laminin-positive cells in the embryonic salivary gland by immunohistologic staining. In 53-day-old embryos, rudiments of salivary glands consist of several large epithelial clusters connected to an epithelial stalk and surrounded by mesenchyme. Laminin was detected throughout the basement membranes of both the clusters and the stalk (Fig. 7A). Intracellular laminin-positive cells were (seen) observed only very slightly in the epithelial clusters and the stalk (arrowhead). In 60-day-old embryonic salivary glands, the epithelium is highly branched, and several terminal lobules and ducts have formed (Fig. 7B). Potent expression of intracellular laminin was observed in epithelial clusters (Fig 7B; arrowhead). In 1-week-old newborns, a well-branched duct system consisting of polarized epithelial cells and ending in the acini was apparent (Fig. 7C). The expression of laminin was observed in the basement membranes of the ducts. Intracellular laminin-positive cells were observed in the periductal area (arrowhead). In 8-year-old adults, the epithelium has differentiated into distinct segments (Fig. 7D). Laminin was detected in the basement membranes, but intracellular laminin was not detected. Intracellular laminin was exclusively expressed in the ep-
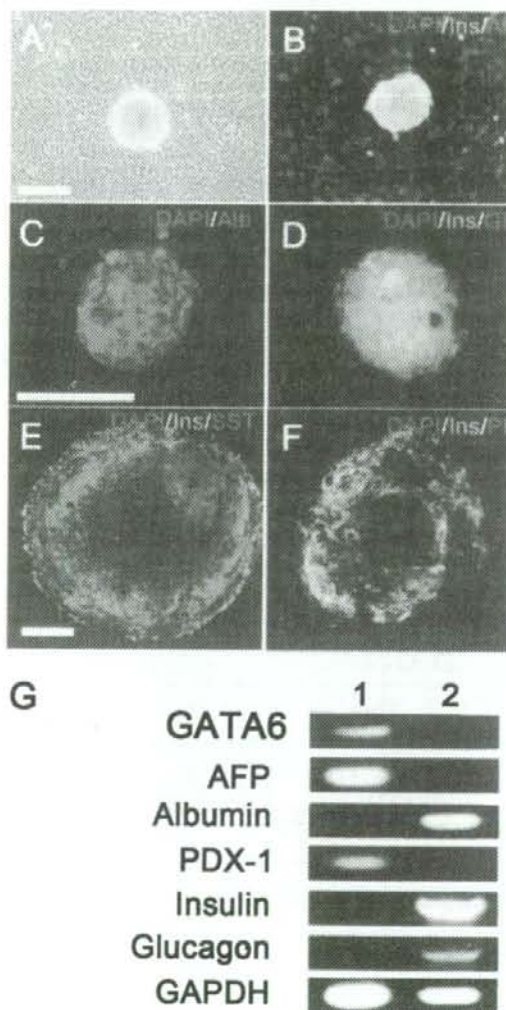

FIG. 4. Immunofluorescent staining and gene analysis of differentiated swine SGP cells. (A) Confluent image of swine SGP cells cultured on plates. Small clusters of cells formed. (B) Albumin (red) and insulin (green) expression was observed in the cells of these small clusters. (C–F) Spheroids of swine SGP cells, which were cultured in the differentiation media in U-bottom plates, were stained by double immunofluorescence staining. Antialbumin (red), anti-insulin (green), antiglucagon (red), antisomatostatin (SST; red), antipancreatic polypeptide (PP; red) antibodies were used. Spheres express (C) albumin (red), (D) insulin (green), (D) glucagon (red). (E,F) For further investigation, stained cells were viewed under a confocal laser-scanning microscope FV500 (Olympus Optical Ltd., Tokyo, Japan). (E) somatostatin (red) and (F) pancreatic polypeptide (red) were detected in spheres. Scale bars: 100 mm. (G) Reverse-transcriptase polymerase chain reaction analyses were performed on messenger RNA obtained from cultured swine SGP cells. Total RNA was isolated. Lane 1: monolayer cultures on type I collagen of swine SGP cells. Lane 2: spheroid bodies of swine SGP cells cultured in U-bottom plates for 7 days. Primers for GATA6, AFP, albumin, PDX-1, insulin, glucagon, and glyceraldehyde-3-phosphate dehydrogenase were used.
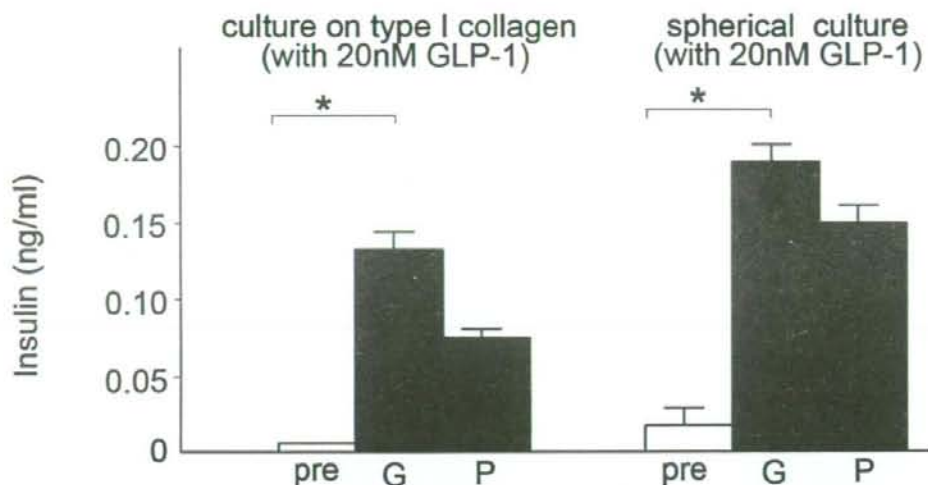
culture on type I collagen
(with 20nM GLP-1)

spherical culture
(with 20nM GLP-1)

FIG. 5. Glucose-stimulation test. (Left) Swine SGP cells were cultured on type I collagen in the differentiation medium with 20 nmol/L GLP-1. (Right) Swine SGP cells were cultured on 96-well U-bottom plate in the medium with 20 nmol/L GLP-1. Pre, swine SGP cells before stimulation; G, high glucose loading (20 mmol/L D-glucose), P, high potassium loading (50 mmol/L potassium). The number of tested cells were corrected. Pancreatic endocrine cells were used for control. $*p < 0.05$, $**p < 0.05$, Mean ± SD.
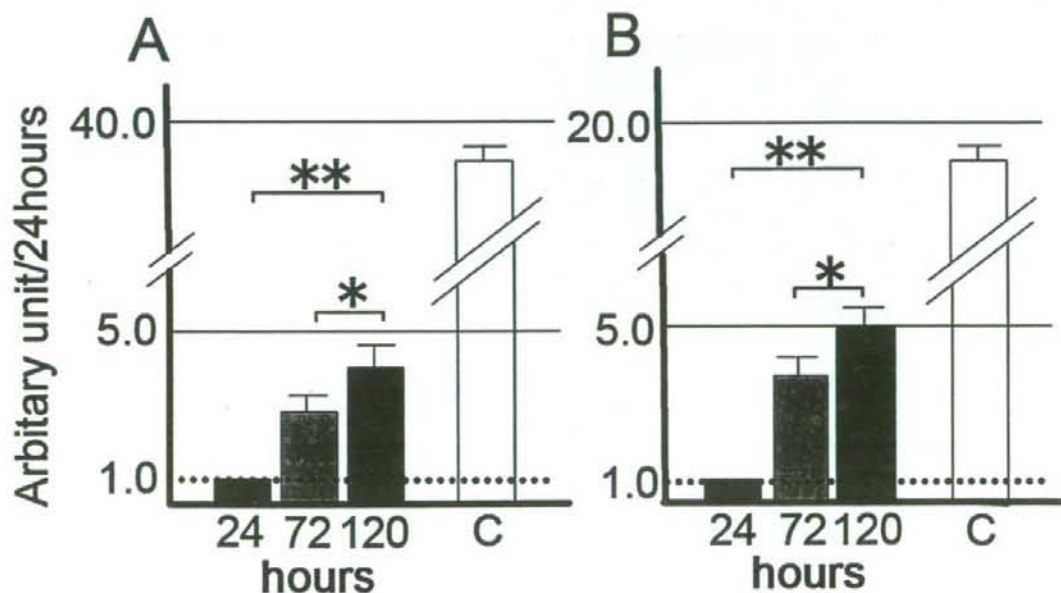

FIG. 6. Quantification of mRNA expression for albumin (A) and insulin (B) in SGP cells with spherical culture by real-time PCR. Quantification was performed 24 h, 72 h, and 120 h after differentiation with spherical culture.$*p < 0.05$, $**p < 0.05$. C, control (A, hepatocytes and pancreatic endocrine cells). Mean ± SD, $n = 5$.
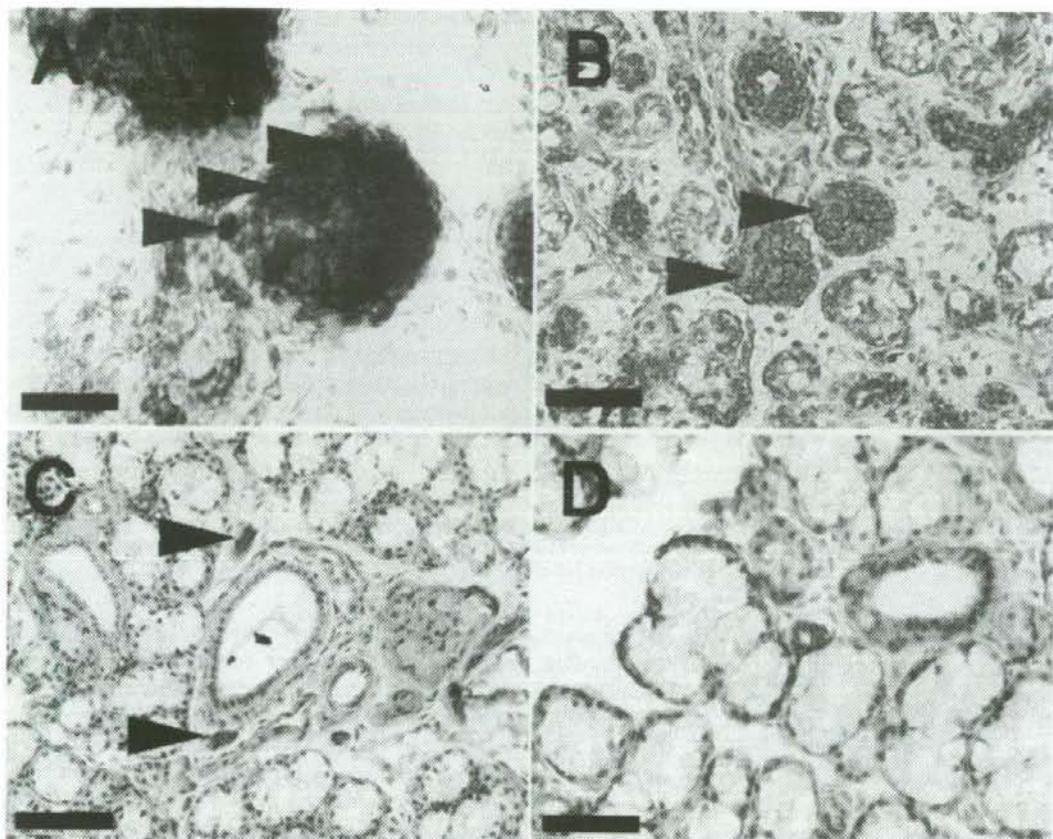
FIG. 7. Expression of laminin in the developing swine salivary gland as shown by immunohistologic staining. (A) On day E53, a continuous distribution of the laminin can be seen in the basement membranes of both the terminal cell clusters and the stalk (arrowhead). (B) On day E60, the expression of laminin is seen in the basement membrane surrounding the ducts, and some of the epithelial cells are positive for intracellular laminin (arrowhead). (D) In neonatal glands, laminin expression is found in the basement membrane of the ducts. The basement membrane of the acini is weakly positive for laminin. Some intracellular laminin-positive cells are found around the periductal area (arrowhead). (D) In adult swine, localization of laminin is evident in basement membranes of both the ducts and acini.

ithelium of the developing salivary gland, as well as in the duct-ligated adult salivary gland.

DISCUSSION

We had previously isolated salivary gland-derived progenitor cells (SGP) from mice and rats. Immunocytochemistry and flow cytometric analysis revealed that mouse and rat SGP-1 cells express CD29, CD44, CD49f, Thy-1, and c-Kit antigen in common. In addition, mouse and rat SGP-1 cells are positive for intracellular laminin. In this study, we successfully isolated progenitor cells

from an injured swine salivary gland with duct ligation. Analysis of surface markers revealed CD29, CD44, CD49f, and Thy-1 antigen expression in swine SGP cells, with some populations also expressing CD49c and c-Kit. In addition, the expression of intracellular laminin was also a common feature in mouse, rat, and swine SGP cells. Swine SGP cells were laminin-1 immunoreactive the same as mouse SGP cells (data not shown). Laminin-1 is the major component of the early embryonic basement membrane, which is required for normal development (Aumailly and Smyth, 1998; Ekblom et al., 1998; Li et al., 2002). By binding to cell-surface integrins, such as $\alpha 6\beta 1$, $\alpha 3\beta 1$,

TABLE 3.   MARKERS IN RAT, MOUSE, AND SWINE SGP CELLS

Stem/ progenitor cell	Localization	Marker protein		Differentiation
		Intracellular	Surface	
Rat SGP-1	duct or periductal area	CK19 Laminin	CD29+, CD34+, CD49f+, CD45−	Liver cells Pancreatic edocrine
Mouse SGP-1	duct or periductal area	CK19 Laminin AFP	CD44+, CD49f+, Sca1+, CD49c+, CD51+, CD45−	Liver cells Pancreatic edocrine
Swine SGP	Duct or periductal area	CK19 CK18 Laminin AFP	CD29+, CD34+, CD44+, CD49f+, CD90(Thy-1)+, CD117(c-kit)+, CD45−	Hepatic phenotypes Pancreatic endocrine Neural phenotypes
Porcine mesenchymal stem cells	Bone marrow		CD29+, CD90(Thy-1)+, CD44+, SLA-l+, CD106+, CD46+, CD45−	Cardiomyocytes Chondrogenic, osteogenic and adipogenic differentiation Neural differentiation?

The expression of intracellular-laminin and CD49f are common antigens among the rat, mouse, and swine SGP cells. Rat and mouse SGP cells are positive for CK19. Swine SGP cells were positive for CK19 in primary culture. AFP express in undifferentiated cells of mouse and swine SGP cells, but not rat SGP cells. Swine SGP cells differentiate into the same hepatic and pancreatic phenotypes as rat and mouse SGP cells.

and $\alpha5\beta1$ integrin, laminins promote cell adhesion and exert profound influence on the proliferation, differentiation, and survival of cells (Dabies, 2002; Delwel and Sonnenberg, 1996; Mercurio, 1995; Tate et al., 2004; Wang et al., 2003). Both Thy-1 and c-Kit antigens are well known stem cell markers expressed on stem cells of the hematopoietic stem cells and hepatic oval cells (Bryon et al., 1998; Craig et al., 1993; Crosby et al., 2001; Petersen et al., 1998; Ryu et al., 2004). These findings indicate the markers of newly isolated swine SGP cells to be quite similar to previously reported SGP cells of rodents, and SGP cells are well conserved in the species.

Immunohistochemistory revealed that monolayer-cultured mouse SGP-1 cells expressed the genes of AFP and CK 19. CK8 and CK18 are markers for hepatocytes, and CK19 is a marker for hepatic progenitor or cholangiocytes. Isolated swine SGP cells were also positive for CK19 and AFP, and were positive for CK18 and AFP in prolonged passages. This phenotypic change of swine SGP cells was observed after 15 passages. It is the reason that we used the swine SGP cells of 7 to 15 passages for the differentiation study. Swine SGP cells can differentiate into insulin and albumin producing cells *in vitro*. Swine SGP cells cultured on type I collagen autonomously formed cell clusters containing insulin and albumin-producing cells. Autonomous differentiation, which depends on cell density, is a common characteristic among SGP cells of the three species. For the

assessment of differentiation, we performed spherical cultures that form a uniform three-dimensional structure. By application of the spherical culture, disappearance of intracellular laminin in swine SGP cells accompanied by emerging laminin immunoreactivity around the cells was observed as rat SGP cells (data not shown). Spherical culture was effective for swine SGP cell differentiation in the same manner as mouse SGP cells. Glucagon-like peptide 1 (GLP-1), derived from intestinal cells, is among the substances that may regulate insulin secretion and cell proliferation (Drucker, 2002; Perfetti and Merkel, 2000). We performed spherical culture with and without GLP-1 to investigate GLP-1 responsibility in the differentiation that is observed in mouse SGP cells. GLP-1 enhanced the differentiation into insulin-producing cells. Meanwhile, swine SGP cells cultured without GLP-1 predominantly differentiate into albumin-producing cells. This finding suggests that swine SGP cells with spherical culture dominantly differentiate into albumin-producing cells, and GLP-1 changes the direction of differentiation from hepatic to pancreatic endocrine phenotypes. The GLP-1 role is interesting, and suggests a common differentiation system among SGP cells. We used porcine PE cells for positive control of insulin secretion. The porcine PE cells consisted mainly of insulin-producing β-cells and have glucose and potassium sensitivity *in vitro*. Swine SGP cells

start to express the insulin gene with the start of spherical culture, and gene expression is augmented during the course of spherical culture. After 7 days in spherical culture, swine SGP cells have insulin production and secretion upon glucose and potassium stimulation.

For investigation of somatic progenitor cells in the salivary gland of mice, rats, and swine, we used tissue injury models with ligation of the main excretory duct. In mice, we demonstrated that mouse SGP-1 cells originated from the proliferated small epithelial cells (Sca-1+/c-Kit+) in duct-ligated salivary gland by FACS sorting. This result indicated that the small epithelial cells contained stem/progenitor cells, and the appearance of intracellular laminin-positive cells were a common feature in the three species. In normal adult salivary glands, intracellular laminin-positive cells are not found. Intracellular laminin-positive cells are observed in embryonic salivary glands. We investigated intracellular laminin-positive cells in duct-ligated salivary glands and embryonic salivary glands by immunohistological staining. Small numbers of laminin-positive cells appeared in the duct-ligated glands of mice and rats. Laminin-positive cells are typically observed in the terminal clusters which appear during development of the salivary gland of mice (Kadoya et al., 1995; Kadoya and Yamashita, 1989; Lazowski et al. 1994). In swine embryonic salivary glands, laminin-positive cells were observed in the terminal clusters. In neonatal salivary glands, some intracellular laminin-positive cells are detected in the periductal area. Intracellular laminin-positive cells were not detected in salivary glands over 8 weeks old (data not shown). Swine, rat, and mouse SGP cells are intracellular laminin immunoreactive but also positive for markers that expressed in mesenchymal stem cells as follows, CD29, CD44, CD49, and Thy-1 antigen. We speculated on the correlation between mesenchymal stem cells and SGP cells (Table 3). It was recently reported that pancreatic stem cells derived from the pancreas duct also express markers attributable to mesenchymal stem cells. Further research for identification of SGP cells is required (Zhang et al., 2003).

ACKNOWLEDGMENTS

REFERENCES

Abe, K., and Watanabe, S. (1995). Apoptosis of mouse pancreatic acinar cells after duct ligation. Arch. Histol. Cytol. 58, 221–229.

Aumailly, M., and Smyth, N. (1998). The role of laminins in basement membrane function. J. Anat.193, 1–21.

Bryon, E.P., Julie, P.G., Joel, S.G., et al. (1998). Hepatic oval cells express the hematopoietic stem cell marker Thy-1 in the rat. Hepatology 27, 433–445.

Caperna, T.J., Failla, M.K., Kornegay, E.T., et al. (1985). Isolation and culture of parenchymal and nonparenchymal cells from neonatal swine liver. J Anim Sci 61, 1576–1586.

Craig, W., Kay, R., Cutler, R.L., et al. (1993). Expression of Thy-1 antigen on human hematopoietic progenitor cells. J. Exp. Med. 177, 1331–1342.

Crosby H.A., Kelly, D.A., and Strain, A.J. (2001). Human hepatic stem-like cells isolated using c-kit or CD34 can differentiate into biliary epithelium. Gastroenterology 120, 534–544.

Dabeva, M.D., Hwang, S.G., Vasa, S.R., et al. (1997). Differentiation of pancreatic epithelial progenitor cells into hepatocytes following transplantation into rat liver. Proc. Natl. Acad. Sci. USA 94, 7356–7361.

Dabies, J.A. (2002). Do different branching epithelial use a conserved developmental mechanism? Bioessays 24, 937–948

Delwel, G.O., and Sonnenberg, A. (1996). Laminin isoforms and their integrin receptors. In Adhesion Receptors as Therapeutic Targets. M.A. Horton, ed. (CRC Press, Boca Raton, FL), pp. 9–36.

Drucker, D.J. (2002). Biological actions and therapeutic potential of the glucagonslike peptides. Gastroenterology 122, 531–544.

Ekblom, M., Falk, M., Salmivirta, K., et al. (1998). Laminin isoforms and epithelial development. Ann. NY Acad. Sci. 857, 194–211.

Fernández-Fígares, I., Shannon, A.E., Wray-Cahen, D., et al. (2004). The role of insulin, glucagon, dexamethasone, and leptin in the regulation of ketogenesis and glycogen storage in primary cultures of porcine hepatocytes prepared from 60 kg pigs. Domest. Anim. Endocrinol. 27, 125–140.

Gillio-Meina. C., Hui, Y.Y., and LaVoie, H.A. (2003). GATA-4 and GATA-6 transcription factors: expression, immunohistochemical localization, and possible function in the porcine ovary. Biol. Reprod. 68, 412–422.

Golding, M., Sarraf, C.E., Lalani, E.N., et al. (1995). Oval cell differentiation into hepatocytes in the acetylaminofluorene-treated regenerating rat liver. Hepatology 22, 1243–1253.

Hisatomi, Y., Okumura, K., Nakamura, K., et al. (2004). Flow cytometric isolation of endodermal progenitors from mouse salivary gland differentiate into hepatic and pancreatic lineages. Hepatology 39, 667–675.

Kadoya, Y., and Yamashina, S. (1989). Intracellular accumulation of basement membrane components during morphogenesis of rat submandibular gland. J. Histochem. Cytochem. 37, 1387–1392.

Kadoya, Y., Kadoya, K., Durbeej, M., et al. (1995). Antibodies against domain E3 of laminin-1 and integrin alpha 6 subunit perturb branching epithelial morphogenesis of submandibular gland, but by different modes. J. Cell Biol. 129, 521–534.

Lazowski, K.W., Merts, P.M., Redman, R.S., et al. (1994). Temporal and spatial expression of laminin, collagen types IV and I and alpha 6/beta 1 integrin receptor in the developing rat parotid gland. Differentiation 56, 75–82.

Li, X., Talts, U., Talts, J.F., et al. (2001). Akt/PKB regulates laminin and collagen IV isotypes of the basement membrane. Proc. Natl. Acad. Sci. 98, 14416–11421.

Mercurio, A.M. (1995). Laminin receptors: achieving specificity through cooperation. Trends Cell Biol. 5, 419–423.

Nagai, K., Tsuchiya, K., Ezaki, T., et al. (2004). Effect fo GLP-1 (glucagon-like peptide 1:7-36 amide) on porcine pancreatic endocrine cell proliferation and insulin secretion. Pancreas 28, 138–145.

Ohgawara, H., Kobayashi, A., Chong, S., et al. (1994). Preparation of adult pig pancreatic cells: comparative study of methods with or without proteolytic enzymes. Cell Transplant 3, 325–331.

Ohgawara, H., Shaken, T., Fukuknaga, K., et al. (1998). Establishment of monolayer culture of pig pancreatic endocrine cells by use of nicotinamide. Diabetes Res Clin Pract, 42, 1–8.

Okumura, K., Nakamura, K., Hisatomi, Y., et al. (2003). Salivary gland progenitor cells induced by duct ligation differentiate into hepatic and pancreatic lineages. Hepatology 38, 104–113.

Omori, M., Evarts, R.P., Omori, N., et al. (1997). Expression of α-fetoprotein and stem cell factor/c-kit system in bile duct ligated young rats. Hepatology 25, 1115–1122.

Perfetti, R., and Merkel, P. (2000). Glucagon-like peptide-1: a major regulator of pancreatic-cell function. Eur. J. Endocrinol. 142, 715–725.

Petersen, B.E., Goff, J.P., Greenberger, J.S., et al. (1998). Hepatic oval cells express the haematopoietic stem cell marker Thy-1 in the rat. Hepatology 27, 433–445.

Richards, M.P., and Poch, S.M. (2002). Quantitative analysis of gene expression by reverse transcription polymerase chain reaction and capillary electrophoresis with laser-induced fluorescence detection. Mol. Biotechnol. 21, 19–37.

Ryu, B.Y., Orwig, K.E., Kubota, H., et al. (2004). Phenotypic and functional characteristics of spermatogonial stem cells in rats. Dev. Biol. 274, 158–151.

Takahashi. S., Schoch, E., and Walker, N.I. (1998).Origin of acinar cell regeneration after atrophy of the rat parotid induced by duct obstruction. Int. J. Exp. Pathol. 79, 293–301.

Tate, M.C., Garcia, A.J., Keselowsky, B.G., et al. (2004). Specific $\beta 1$ integrins mediate adhesion, migration, and differentiation of neural progenitors derived from the embryonic striatum. Mol. Cell. Neurosci. 27, 22–31.

Walker, N.I. (1987). Ultrastructure of the rat pancreas after experimental duct ligation. I. The role of apoptosis and intraepithelial macropharges in acinar cell deletion. Am. J. Pathol. 126, 439–451.

Walker, N.I., and Gobe, G.C. (1987). Cell death and cell proliferation during atrophy of the rat parotid gland induced by duct obstruction. J. Pathol. 153, 333–344.

Wang, H.J., Pieper, J., Schotel, R., et al. (2004). Stimulation of skin repair is dependent on fibroblast source and presence of extracellular matrix. Tissue Eng. 10, 1054–1064.

Wang, R.N., Klöppel, G., and Bouwens, L. (1995). Duct-to islet-cell differentiation and islet growth in the pancreas of duct-ligated adult rats. Diabetologia 38, 1405–1411.

Yang, L., Li, S., Hatch, H., et al. (2002). In vitro trans-differentiation of adult hepatic stem cells into pancreatic endocrine hormone-producing cells. Proc. Natl. Acad. Sci. USA 99, 8078–8083.

Yasui, O., Miura, N., Terada, K., et al. (1997). Isolation of oval cells from Long-Evans Cinnamon rats and their transformation into hepatocytes in vivo in the rat liver. Hepatology 25, 329–334.

Zhang, J., Niu, C., Ye, L., et al. (2003). Identification of the haematopoietic stem cell niche and control of the niche size. Nature 425, 836–841.

Address reprint requests to:
Fumio Endo, MD, PhD
Department of Pediatrics
Kumamoto University School of Medicine
Honjo 1-1-1
Kumamoto 860-8556, Japan

E-mail: fendo@kumamoto-u.ac.jp

Arrhythmia induced by spatiotemporal overexpression of calreticulin in the heart

Kiyoko Hattori [a], Kimitoshi Nakamura [a,*], Yuichiro Hisatomi [a], Shirou Matsumoto [a,1],
Misao Suzuki [b], Richard P. Harvey [c,d], Hiroki Kurihara [e], Shinzaburo Hattori [a],
Tetsuro Yamamoto [f], Marek Michalak [g], Fumio Endo [a]

[a] Department of Pediatrics, Graduate School of Medical Science, Kumamoto University, Japan
[b] Division of Transgenic Technology, Center for Animal Resources and Development, Kumamoto University, Japan
[c] Victor Chang Cardiac Research Institute, Australia
[d] Faculties of Medicine and Life Sciences, University of New South Wales, Australia
[e] Department of Physiological Chemistry and Metabolism, Graduate School of Medicine, The University of Tokyo, Japan
[f] Department of Molecular Pathology, Faculty of Medical and Pharmaceutical Sciences, Kumamoto University, Japan
[g] Membrane Protein Research Group, Department of Biochemistry, University of Alberta, Edmonton, Alta., Canada

ELSEVIER

Arrhythmia induced by spatiotemporal overexpression of calreticulin in the heart

Kiyoko Hattori [a], Kimitoshi Nakamura [a,*], Yuichiro Hisatomi [a], Shirou Matsumoto [a,1],
Misao Suzuki [b], Richard P. Harvey [c,d], Hiroki Kurihara [e], Shinzaburo Hattori [a],
Tetsuro Yamamoto [f], Marek Michalak [g], Fumio Endo [a]

[a] *Department of Pediatrics, Graduate School of Medical Science, Kumamoto University, Japan*
[b] *Division of Transgenic Technology, Center for Animal Resources and Development, Kumamoto University, Japan*
[c] *Victor Chang Cardiac Research Institute, Australia*
[d] *Faculties of Medicine and Life Sciences, University of New South Wales, Australia*
[e] *Department of Physiological Chemistry and Metabolism, Graduate School of Medicine, The University of Tokyo, Japan*
[f] *Department of Molecular Pathology, Faculty of Medical and Pharmaceutical Sciences, Kumamoto University, Japan*
[g] *Membrane Protein Research Group, Department of Biochemistry, University of Alberta, Edmonton, Alta., Canada*

Abstract

Calreticulin (CRT) is a Ca^{2+}-binding protein of the endoplasmic reticulum essential for cardiac development. For further investigation of the functional mechanism of calreticulin, we generated transgenic mice with spatiotemporal overexpression of calreticulin using a cre-loxP system. To elucidate the role of the protein in cardiogenesis, we adopted Nkx2.5-cre mice for heart specific overexpression. The overexpression of calreticulin was associated with arrhythmia, chamber dilation and sudden death, as observed in 6- to 10-week-old mice. Furthermore, transgenic mice displayed marked edema at 7-weeks of age. RT-PCR analysis revealed that the expression of hyperpolerization-activated cyclic nucleotide-gated channel1 (HCN1), an essential component for cardiac pace maker activity, had receded in the heart of transgenic mice. In addition, the protein level of connexin40 (Cx40), connexin43 (Cx43), components of gap junction, and myocyte-enhancer factor (MEF) 2C, a cardiac-specific transcriptional factor, were reduced in the transgenic mice hearts. These findings suggest that calreticulin affects cardiac arrhythmia with disruption of cardiac signaling, such as the HCN family members, and with low levels of Cx40 and Cx43. Overepression of calreticulin also leads to a decreased protein level of MEF2C and this may cause changes in cardiac structure. Our findings support calreticulin being critical for normal heart function and structure. These mice are a useful model for the study of endoplasmic reticulum proteins, such as calreticulin, in various tissues.
© 2007 Elsevier Inc. All rights reserved.

Keywords: Calreticulin; Overexpression; Arrhythmia; Sudden death; Cardiac edema; HCN1; MEF2C

Introduction

Calreticulin (CRT) is a Ca^{2+}-binding chaperone, which is resident in the lumen of the endoplasmic reticulum and plays a critical role in the regulation of Ca^{2+} homeostasis. Calreticulin and other Ca^{2+}-binding proteins such as

Grp94, BiP, PDI, and ERp72 participate in the synthesis of a variety of molecules including ion channels, surface receptors, integrins and transporters. Calreticulin also has various functions, such as regulation of apoptosis, cell adhesion, Ca^{2+}-dependent transcriptional process [1,2], etc. Ca^{2+}-signaling participates in multicellular stages of the generation of the basic embryonic pattern and the differentiation of key organ systems, such as the nervous system, heart, muscle and kidney [3]. Calreticulin is highly expressed in the developing heart, but is only a minor

* Corresponding author. Fax: +81 96 366 3471.
E-mail address: kimnak@kaiju.medic.kumamoto-u.ac.jp (K. Nakamura).
[1] The Japan Society for the Promotion of Science Research fellow.

component of the mature heart [4]. It is demonstrated that the expression of calreticulin affects the heart development and its function. Calreticulin-deficient mice die as embryos and exhibit impaired cardiac development characterized by a marked decrease in ventricular wall thickness and deep intertrabecular recesses in the ventricular wall [4]. The development of the heart may require the Ca^{2+}-dependent signaling pathways, such as the calreticulin/calcineurin/NF-AT/GATA-4 transcription pathway and/or calreticulin/calcineurin/MEF2C transcription pathway [4–6].

The transgenic mice overexpressing calreticulin in the heart driven by the cardiac α myosin heavy chain (α-MHC) promoter exhibited sinus bradycardia, complete heart block and sudden death [7]. The study indicates that a calreticulin related abnormality might have a role in the dysfunction of conduction system.

In this study, we have generated transgenic mice with spatiotemporal overexpression of calreticulin using a cre-loxP system. The transgenic mice exhibited extrinsic expression of calreticulin in the liver or in the heart driven by tissue specific cre recombination. In particular, we have adopted Nkx2.5 promoter-cre mice which display overexpression of calreticulin at early stage of heart development. Nkx2.5 is a member of the Nkx homeobox gene family, and Nkx2.5 expression starts 7.5 days postcoitus in the precardiac mesoderm and its expression is maintained even in the adulthood [8,9]. These transgenic mice shed light on the role of calreticulin by alterations of the expression level in the heart. These transgenic mice display arrhythmia, chamber dilation and sudden death at 6- to 10-weeks of age. These transgenic mice are unique among the animal models for arrhythmia. Furthermore, they are useful for analysis of the role of endoplasmic reticulum proteins, such as calreticulin, in the regulation of various tissue functions.

Materials and methods

Generation of the Nkx2.5-CRT transgenic mice

The pBL-CAG-loxP-CAT-loxP-Rabbit β-globin polyA plasmid (a gift from Ms. Kimi Araki of Kumamoto University) was ligated with the plasmid CRT cDNA gene, which was cut from pcD-CRT-HA plasmid [7] by EcoRI and XbaI site to generate the transgene vector containing a CAG promoter-loxP-CAT gene-loxP-CRT cDNA. This plasmid pBL-CAG-loxP-CAT-loxP-CRT cDNA was cut by SalI and SmaI, and was used as a transgene to make loxP-CRT transgenic mice. The loxP-CRT transgenic mice were made by microinjection of this transgene into pronuclear cells of C57BL/6 mice that were subsequently transferred to pseudopregnant foster females.

The loxP-CRT transgenic mice were cross-bred with Nkx2.5-cre mice to generate transgenic mice with cardiac specific overexpression of calreticulin (Nkx2.5-CRT transgenic mice). Nkx2.5-cre mice express cre recombinase under the control of the Nkx2.5 promoter. The loxP-CRT transgenic mice were also cross-bred with albumin-cre mice (The Jackson Laboratory, Bar Harbor, USA) to generate other transgenic mice with hepatic specific overexpression of calreticulin (albumin-CRT transgenic mice). The NKx2.5-CRT transgenic mice and the albumin-CRT transgenic mice were genotyped by PCR using the following primers. The primers for

detecting the CAT gene were CAT1 (5′-TCACTGGATATACCAC CGTT-3′) and CAT2 (5′-CGAAAAACATATTCTCAATA-3′). The primers for detecting the cre recombinase gene were cre1 (5′-ACATG TTCAGGGATCGCCAG-3′) and cre2 (5′-TAACCAGTGAAACAGC ATTGC-3′). The protocol was approved by the Center for Animal Resources and Development of Kumamoto University. Animal care was performed as outlined in the Guide for Care and Use of Laboratory Animals.

Western blot analysis

Western blot analyses were performed as previously described [7]. Blots were probed with polyclonal rabbit anti-HA (1:200, Santa Cruz Biotechnology, Inc., Santa Cruz, CA), polyclonal goat anti-calreticulin (1:3000) [7,10], monoclonal mouse anti-connexin43 (1:1000, Chemicon International, Inc., Temecula, CA), polyclonal rabbit anti-connexin40 (1:100, Zymed Laboratories, San Francisco, CA, USA), polyclonal goat anti-MEF2C (1:200, Santa Cruz) or polyclonal rabbit anti-GAPDH (1:200, Santa Cruz), followed by corresponding horseradish peroxidase-conjugated secondary antibodies including swine anti-rabbit immunoglobulins HRP (1:3000, DAKO Cytomation, Glostrup, Denmark), rabbit anti-goat immunoglobulins HRP (1:12500, DAKO), rabbit anti-mouse immunogloblins HRP (1:2000, DAKO). To determine the quantity of the expression of calreticulin in the heart or in the liver, the blots were analyzed for densitometry using NIH image (Ver1.34s).

Immunostaining of tissues

The sections of harvested tissues for hematoxylin-eosin , periodic acid Schiff (PAS), Gitter staining or immunofluorescent staining were prepared as described previously [11,12]. The primary antibody used in this study was polyclonal rabbit anti-connexin40 (1:100, Zymed). The secondary antibody was Alexa594-conjugated anti-rabbit IgG. (1:100, Molecular Probes, Inc. Eugene, Oregon).

Electron microscopy

For electron microscopic observations, approximately 1 mm^3 of sections of the heart were removed and the sections were prepared as described previously [13].

Electrocardiography

Four-lead ECGs were recorded using surface electrodes attached to the limbs of mice. ECGs were recorded in fully awake mice using a Softron ECG Processor SP2000 (Softron. Co., Ltd, Tokyo, Japan). After the recording was taken, heart rate, the PR and QRS intervals were analyzed. Each value was calculated the average of five recordings per one mouse.

RNA isolation and RT-PCR analysis

Total RNA was extracted from the heart and complementary DNA was prepared as described previously [12]. The resulting complementary DNA was amplified with the following sets of primers: HCN1 (forward: 5′-CTCTTTTTGCTAACGCCGAT-3′, reverse: 5′-CATTGAAATTGT CCACCGAA-3′), HCN2 (forward: 5′-GTGGAGCGAGCTCTACTCG T-3′, reverse: 5′-GTTCACAATCTCCTCACGCA-3′), HCN4 (forward: 5′-GTACGCATCGTGAACCTCATTG-3′, reverse: 5′-TTTCGGCAGT TAAAGTTGATG-3′), Cx40 (forward: 5′-TTTGGCAAGTCACGGCA GGG-3′, reverse: 5′-TGTCACTATGGTAGCCCTGAG-3′), Cx43 (forward: 5′-GGGCAAACCAATTCCACCACC-3′, reverse: 5′-CAAGATT AAATCCAGACGGAG-3′), α-cardiac actin (forward: 5′-TATGCCA ACAATGTCCTAT-3′, reverse: 5′-CACAATACGGTCATCCTGAA-3′), GAPDH (forward: 5′-GGGTGGAGCCAAACGGGTC-3′, reverse: 5′-G GAGTTGCTGTTGAAGTCGCA-3′).

Quantitative real-time PCR

cDNA was prepared as described in *RNA isolation and RT-PCR analysis.* mRNA levels of various genes were quantified by SYBR Green incorporation (SYBR® Premix Ex Taq™; TAKARA BIO Inc., Shiga, Japan) on ABI Prism 7500 Sequence Detection System (Applied Biosystems) and were normalized to glyceraldehydes-3-phosphate dehydrogenase (GAPDH) housekeeping genes. The primers used for gene amplification for real-time PCR were as follows: GAPDH (forward: 5'-C CTGCACCACCAACTGCTTA-3', reverse: 5'-TCATGAGCCCTTCCA CAATG-3'), BNP (forward: 5'-CACCGCTGGGAGGTCACT-3', reverse: 5'-GTGA GGCCTTGGTCCTTCAA-3'), ANP (forward: 5'-TT CTTCCTCGTCTTGGCCTTT-3', reverse: 5'-GACCTCATCTTCTAC CGGCA TCT-3'), β-MHC (forward: 5'-TACCTCATGGGGCTGAAC TC-3', reverse: 5'-C CCTTGGTGACGTACTCGTT-3'), α-MHC (forward: 5'-GGCACAGAAGATGCTGACAA-3', reverse: 5'-CTGCCCCTT GGTGACATACT-3').

Apoptosis assay

Apoptosis was detected with the TUNNEL method using an ApopTag Plus *in situ* apoptosis detection kit (Intergen Company, Purchase, NY, USA), according to the manufacturer's instructions.

Statistical analysis

Variables were compared between NKx2.5-CRT transgenic mice and control mice by Student's *t*-test or Mann–Whitney *U*-test using statistical software (SPSS and Excel). A value of *P* < 0.05 was considered statistically significant. The data shown are means ± SEM.

Results

Generation of transgenic mice

To generate the mice overexpressing calreticulin in specific tissue using a cre-loxP system, loxP-CRT transgenic mice were cross-bred with tissue specific-cre mice (Fig. 1a). The genotypes were identified after PCR analysis of genomic DNA using the sets of primers for the loxP-CRT transgene or the cre recombinase transgene. By intercrossing the loxP-CRT transgenic mice with the albumin-cre mice, we generated the transgenic mice with overexpression of calreticulin, especially in the liver. Calreticulin originating from the transgene was detected by the expression of an HA tag inserted in the loxP-CRT transgene. Western blot analysis probed with anti-HA antibodies revealed that extrinsic calreticulin was specifically expressed in the liver of albumin-CRT transgenic mice (Fig. 1b). Western blot analysis using anti-calreticulin antibodies revealed that the hepatic calreticulin protein levels of albumin-CRT transgenic mice were increased by 1.5-fold compared with control mice (Fig. 1c).We thus confirmed that tissue-specific overexpression of calreticulin is achieved by using a cre-loxP system of the transgenic mice.

Next, to elucidate the role of the calreticulin in cardiogenesis, we generated the transgenic mice with cardiac specific
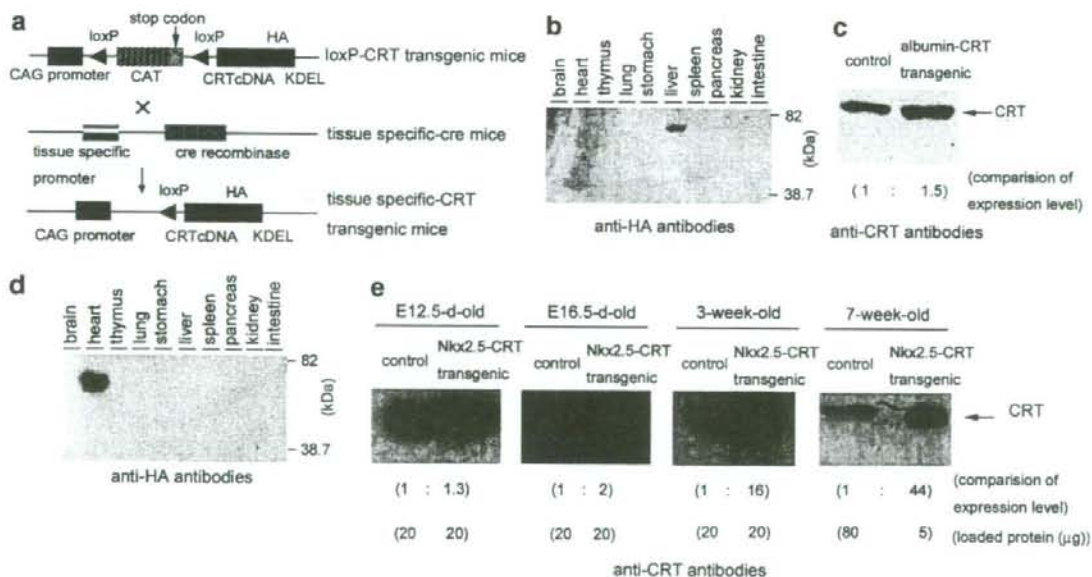
Fig. 1. Construction of the transgene and generation of tissue specific overexpression of calreticulin transgenic mice with western blot analysis of proteins extracted from control and transgenic mice. (a) The conditional transgenic loxP-CRT transgene consists of a CAG promoter, a loxP-flanked CAT gene, followed by CRT cDNA (top). Tissue specific-cre mice express cre recombinase under the control of the tissue specific promoter (middle). The loxP-CRT transgenic mice are cross-bred with tissue specific-cre mice to generate transgenic mice with tissue specific overexpression of calreticulin. Tissue specific-cre mediated recombination excises the floxed CAT gene, resulting in the expression of calreticulin (bottom). (b and d) Western blot analysis probed with anti-HA antibodies revealed extrinsic expression of CRT in the liver of albumin-CRT transgenic mice (b) and in the heart of Nkx2.5-CRT transgenic mice (d). (c and e) Overexpression of calreticulin was shown in the Western blot analysis of the liver from albumin-CRT transgenic mice (c) and the heart from Nkx2.5-CRT transgenic mice (e) probed with anti-calreticulin antibodies. The hepatic calreticulin protein level of the albumin-CRT transgenic mice was increased by 1.5-fold compared with control mice (c). The cardiac calreticulin protein levels of the Nkx2.5-CRT transgenic mice at E12.5-d-old, E16.5-d-old, 3- and 7-week-old were increased by1.3-, 2.0-, 16-and 44-fold compared with control mice, respectively (e).

overexpression of calreticulin by intercrossing the loxP-CRT transgenic mice with the Nkx2.5-cre mice. The number of the Nkx2.5-CRT transgenic mice pups obtained was similar to wild type mice and the transgenic mice with the loxP-CRT or Nkx2.5-cre transgene. The ratio of wild type: loxP-CRT$^+$/Nkx2.5-cre$^-$: loxP-CRT$^-$/Nkx2.5-cre$^+$: loxP-CRT$^+$/Nkx2.5-cre$^+$ genotypes (1:0.7:0.9:0.9, $n = 218$) was close to Mendelian, indicating little or no reduction in viability due to the overexpression of calreticulin. Western blot analysis with anti-HA antibodies revealed that calreticulin of transgene origin was specifically expressed in the heart of the Nkx2.5-CRT transgenic mice (Fig. 1d). The cardiac calreticulin protein levels of the Nkx2.5-CRT transgenic mice at E12.5-d-old, E16.5-d-old, 3- and 7-week-old were increased by 1.3-, 2.0-, 16-and 44-fold compared with control mice, respectively (Fig. 1e). There were no visible macroscopical differences between the Nkx2.5-CRT transgenic and the control mice at E16.5-d-old and 3-week after birth. The Nkx2.5-CRT transgenic mice exhibited a normal increase in body weight until 6-weeks of age (Table 1). However, the Nkx2.5-CRT transgenic mice began to show decreased spontaneous activity as compared with control mice. The onset of the symptom usually preceded death by 2–

Table 1
Comparison of body and heart weight in control and Nkx2.5-CRT transgenic mice

	Control	Nkx2.5-CRT transgenic
Body weight (g)		
Male	19.8 ± 1.7 ($n = 9$)	18.4 ± 1.5 ($n = 11$)
Female	17.2 ± 1.3 ($n = 12$)	17.2 ± 2.6 ($n = 9$)
Heart weight (mg)	66.9 ± 1.7 ($n = 3$)	60.6 ± 5.8 ($n = 3$)

There were not statistical significant for all above comparisons. The body and heart weight were measured at 6- and 7-weeks of age, respectively.

3 days. The Nkx2.5-CRT transgenic mice underwent sudden death after 6-weeks of age and 50% were dead by 8-weeks (Fig. 2b). A portion of the Nkx2.5-CRT transgenic mice exhibited severe systemic edema around 7-weeks of age (Fig. 2a). At the end stage, the Nkx2.5-CRT transgenic mice were very fragile, as several died suddenly from minor stress.

The Nkx2.5-CRT transgenic mice display chamber dilation and systemic congestion

The gross anatomical morphology of the heart of the Nkx2.5-CRT transgenic mice was investigated in E16.5 d-
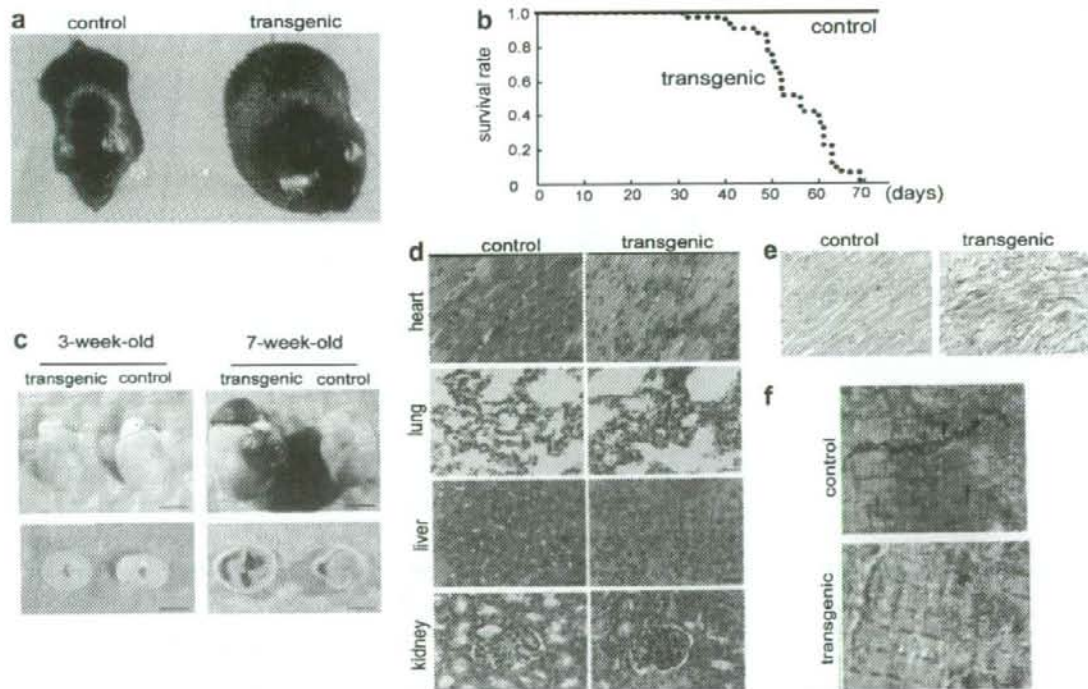

Fig. 2. Phenotype, morphological and pathological analysis of the Nkx2.5-CRT transgenic mice. (a) Phenotypes of a control mouse (left) and transgenic mouse (right) at 7-weeks of age are shown in (a). (b) Survival time of the transgenic mice was analyzed by Kaplan-Meier estimate. The transgenic mice underwent sudden death after 6-weeks. (c) Representative hearts from aged control and the transgenic mice (3-week-old, left, and 7-week-old, right) are shown in (c). Scale bars = 3 mm. (d) Sections from control and the transgenic hearts, lungs, livers and kidneys at 7-weeks of age were stained with hematoxylin and eosin. Scale bars = 20 μm. (e) Gitter-stained sections taken from the hearts of control (left) and Nkx2.5-CRT transgenic mice (right). Scale bars = 20 μm. (f) Electron microscopy of control and the Nkx2.5-CRT transgenic mouse hearts at 7-weeks of age. The arrowhead and black arrows in the section of control mouse indicate the intercalated disk and M-line, respectively. The M-line was frequently absent in sarcomeres of the transgenic mouse hearts (white arrows). The transgenic mouse hearts also have less intercalated disks compared with control mouse. Scale bars = 1 μm.

old, 1-, 3-, 5- and 7-week-old. The Nkx2.5-CRT transgenic mice did not display any abnormalities in the heart up to the 3-week-old (Fig. 2c left). However, after 5-weeks of age, both the atrium and ventricles had expanded compared with the control mice (Fig. 2c right). There was no difference in heart weight between the Nkx2.5-CRT transgenic and control mice at 7-weeks of age (Table 1). Histological examinations of hearts in 7-week-old mice were performed with hematoxylin-eosin staining, PAS staining, and Gitter staining. The staining intensity revealed more heterogeneity in fibers from the Nkx2.5-CRT transgenic mice, and the fibers appear thinner and less compact, but without inflammation, in the transgenic mice heart (Fig. 2d). Gitter staining revealed the presence of interstitial fibrosis in the transgenic heart (Fig. 2e). There was no difference in the number of the PAS positive cells between the Nkx2.5-CRT transgenic and control mice (data not shown). In addition, we investigated sections of the lung, liver and kidney in 7-week-old mice with hematoxylin-eosin staining. Each organ

in the Nkx2.5-CRT transgenic mice exhibited interstitial congestion, but there was no significant morphological change, neither necrosis nor degeneration of the tissue (Fig. 2d). Sarcomeres from the Nkx2.5-CRT transgenic mice hearts were examined by electron microscopy (Fig. 2f). The M-line was frequently absent in sarcomeres from the ventricle of the transgenic mice. Electron microscopy also revealed that the Nkx2.5-CRT transgenic mouse hearts have less intercalated disks compared with control mouse hearts. There was no structural alteration in mitochondria from the transgenic heart in comparison to control. These changes in sarcomere architecture seem to be characteristic for the dilated and the failing heart [14]. As shown in Fig. 3a, the transgenic hearts showed significantly increased both atrial natriuretic peptide (ANP) and brain natriuretic peptide (BNP) mRNA levels, which are marker genes for heart failure. Hypertrophy-associated marker genes such as α-MHC and β-MHC were not induced in the transgenic mice compared with control mice (Fig. 3a). It is thought
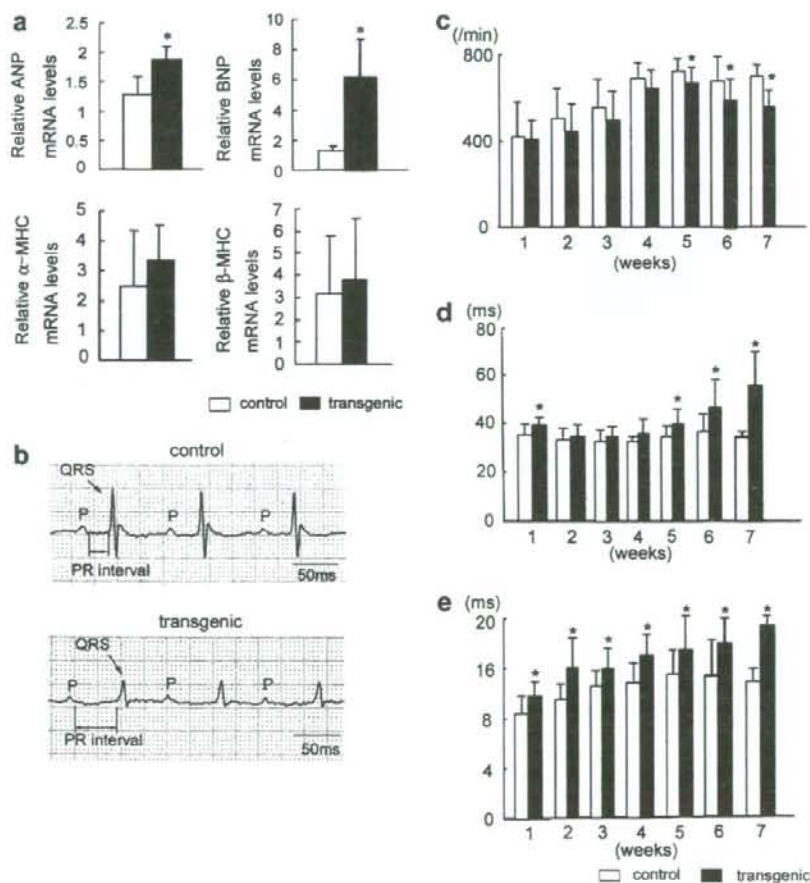

Fig. 3. Quantitative real-time PCR and electrocardiographic analysis of control and the transgenic mice. (a) Relative mRNA expression of the indicated genes in control and the transgenic mice at 7-weeks of age (n = three hearts/group). (b) Representative four-lead ECG from control and the transgenic mice at 7-week-old is shown in (b). (c–e) We compared the heart rate (c), PR interval (d) and QRS interval (e) of the transgenic mice with control mice. *$P < 0.05$ compared to control mice.